

Configuration interaction method for Fock-Darwin states

Andreas Wensauer,^{1,2} Marek Korkusiński,¹ and Paweł Hawrylak¹

¹*Institute for Microstructural Sciences,*

National Research Council of Canada, Ottawa, Canada, K1A 0R6

²*Institut für Theoretische Physik, Universität Regensburg, D-93051 Regensburg, Germany*

Abstract

We present a configuration interaction method optimized for Fock-Darwin states of two-dimensional quantum dots with an axially symmetric, parabolic confinement potential subject to a perpendicular magnetic field. The optimization explicitly accounts for geometrical and dynamical symmetries of the Fock-Darwin single-particle states and for many-particle symmetries associated with the center-of-mass motion and with the total spin. This results in a basis set of reduced size and improved accuracy. The numerical results compare well with the quantum Monte Carlo and stochastic variational methods. The method is illustrated by the evolution of a strongly correlated few-electron droplet in a magnetic field in the regime of the fractional quantum Hall effect.

PACS numbers: 71.15.-m (Methods of electronic structure calculations), 73.21.La (Quantum dots), 73.23.Hk (Coulomb blockade, single electron tunnelling)

INTRODUCTION

In the configuration interaction (CI) method the Hamiltonian of an interacting system is calculated in the basis of many-electron configurations and diagonalized exactly. Unlike the correlated basis of Jastrow or Hylleraas functions, the CI basis functions do not automatically include correlations among pairs of electrons, so their repulsive interaction is not minimized. Hence the size and choice of the basis influences the accuracy of results. Exact diagonalization (ED) has been an important tool used to investigate the electronic and optical properties of quantum dots [1, 2, 3, 4, 5, 6, 7, 8, 9, 10, 11, 12, 13, 14, 15, 16, 17, 18, 19, 20, 21, 22, 23, 24, 25]. Not only does it provide benchmark results for the ground state energy and wave function, but also it gives access to excited states and hence permits an interpretation of a number of spectroscopic techniques such as far-infrared [11], photoluminescence [14], and Raman [15]. In contrast, the quantum Monte Carlo (QMC) [26, 27, 28, 29, 30, 31, 32, 33, 34], mean-field Hartree-Fock [35, 36], and density-functional theory (DFT) calculations [37, 38, 39, 40, 41, 42] are restricted to the ground-state properties.

The objective of this work is to present a CI method optimized for the specific problem of interacting electrons in a parabolic dot in a magnetic field. The optimization explicitly accounts for geometrical and dynamical symmetries of single-particle states, and for many-particle symmetries associated with the center-of-mass (CM) motion and total spin. This results in a reduced basis size and improved accuracy, which in turn allows for a reliable computation of dot properties in the strongly correlated regime. Previous work on total spin and CM-resolved calculations used either the group-theoretical approach limited to a small number of electrons [5, 7], or the lowest Landau level approximation [10]. Here we build on these results to construct a reliable and versatile computational tool capable of testing many of the interesting predictions involving electronic correlations in quantum dots. The paper is organized as follows. In Sec. II we focus on the physical properties of our system, discuss the Hamiltonian, its symmetries and quantum numbers, and its scaling properties. In Sec. III we present a total spin- and CM-resolved CI technique. We compare our results with QMC and stochastic-variational method (SVM) and with previous results describing the evolution of the electronic droplet with the magnetic field.

HAMILTONIAN AND SYMMETRIES

We consider a two-dimensional quantum dot with a parabolic confinement potential of strength ω_0 (henceforth $\hbar = 1$) in a perpendicular magnetic field $\mathbf{B} = (0, 0, B)$. The Hamiltonian for N particles in real-space representation [with $\mathbf{r} = (x, y)$, $\hat{\mathbf{p}} = (\hat{p}_x, \hat{p}_y)$, and the vector potential $\mathbf{A}(\mathbf{r}) = B/2(-y, x)$] is:

$$\hat{H} = \sum_{j=1}^N \left(\frac{1}{2m^*} (\hat{\mathbf{p}}_j + e\mathbf{A}(\mathbf{r}_j))^2 + \frac{1}{2} m^* \omega_0^2 \mathbf{r}_j^2 \right) + \frac{1}{2} \sum_{j,k=1}^N' \frac{e^2}{4\pi\varepsilon\varepsilon_0 |\mathbf{r}_j - \mathbf{r}_k|}, \quad (1)$$

with the Zeeman term omitted for simplicity. Here m^* , e are the electronic effective mass and charge, respectively, $\omega_c = eB/m^*$ is the cyclotron energy, and ε is the dielectric constant of the host semiconductor. We can rewrite the one-particle contribution of equation (1) to obtain $(\mathbf{p}_j^2/2m^* + m^* \omega_h^2 \mathbf{r}_j^2/2 + (\omega_c/2)\hat{l}_j)$, where $\omega_h = \sqrt{\omega_0^2 + \omega_c^2/4}$ is the hybrid frequency and \hat{l}_j is the angular momentum operator. Introducing the effective length $l_h^{-2} = m^* \omega_h$, and scaling all lengths in the units of l_h and energies in effective Rydbergs $Ry = m^* e^4 / 2\varepsilon^2$ results in a dimensionless Hamiltonian,

$$\hat{H} = \frac{1}{(l_h/a_0)^2} \left(\sum_{j=1}^N \left(-\nabla_j^2 + \mathbf{r}_j^2 + \frac{l_h^2}{l_0^2} \hat{l}_j \right) + (l_h/a_0) \sum_{j,k=1}^N' |\mathbf{r}_j - \mathbf{r}_k|^{-1} \right). \quad (2)$$

Here the strength of Coulomb interactions is proportional to the effective length (l_h/a_0) , with $a_0 = \varepsilon/m^* e^2$ being the effective Bohr radius and $l_0^{-2} = m^* \omega_c$ being the magnetic length. Therefore, the larger the effective length or the smaller the hybrid frequency, the larger the contribution from electron-electron interactions.

The Hamiltonian (1) exhibits another scaling property. To see it we rewrite it as a function of ω_0 , ω_c , and N and separate the contribution of the angular momentum. This concept is similar to the modification of the Hamiltonian of a (natural) atom in Ref. [47].

$$\hat{H} = \sum_{j=1}^N \left(\frac{\hat{\mathbf{p}}_j^2}{2m^*} + \left(\omega_0^2 + \frac{\omega_c^2}{4} \right) \frac{m^* \mathbf{r}_j^2}{2} \right) + \sum_{j,k=1}^N' \frac{e^2}{8\pi\varepsilon\varepsilon_0 |\mathbf{r}_j - \mathbf{r}_k|} + \sum_{j=1}^N \frac{\omega_c}{2} \hat{l}_j. \quad (3)$$

The total Hamiltonian is therefore a sum of a Hamiltonian of a dot in zero magnetic field with the confinement frequency $\sqrt{\omega_0^2 + \omega_c^2/4}$, and the total angular momentum contribution $(\omega_c/2)\hat{L}$. As a result we can map the spectra and wave functions of a dot in the presence of the magnetic field to those at zero field. Note that Eq. (3) implies that the energy levels of subspaces with different angular momenta are shifted against each other due to the term

$(\omega_c/2)\hat{L}$, whereas within a specific subspace of the angular momentum the energy levels are fixed relative to each other. Therefore, ground states in high magnetic fields are excited states in zero field and a suitable choice of a finite basis is not trivial.

The choice of the basis is facilitated by the properties of the one- and the many-particle Hamiltonian. The properties of the one-electron Hamiltonian are easily understood by a transformation from the momentum and position representation $(\hat{\mathbf{p}}, \mathbf{r})$ into the language of harmonic-oscillator raising and lowering operators [5, 7]:

$$\hat{H}_0 = \omega_+(\hat{a}_+^\dagger \hat{a}_+ + 1/2) + \omega_-(\hat{a}_-^\dagger \hat{a}_- + 1/2), \quad (4)$$

with the energy spectrum $\varepsilon_{nm\sigma} = \omega_+(n+1/2) + \omega_-(m+1/2)$ ($n, m = 0, 1, \dots, \infty$), and the two oscillator frequencies $\omega_\pm = \omega_h \pm \omega_c/2$. The harmonic-oscillator spectrum is equivalent to the spectrum derived independently by Fock [44] and Darwin [45] (the Fock-Darwin spectrum, FD) applying different methods. The corresponding states are denoted by $|nm\sigma\rangle$, where $\sigma = \uparrow, \downarrow$ denotes the electronic spin. The eigenvalues of the angular momentum operator $\hat{l} = \hat{n} - \hat{m}$, the spin $\hat{\mathbf{s}}^2$, and its z -component \hat{s}_z are good quantum numbers. In addition, there are dynamical symmetries associated with the form of the confining potential. These symmetries lead to degeneracies of the harmonic-oscillator spectrum at $B = 0$ and also at finite fields whenever $\omega_+/\omega_- = k$, with $k = 1, 2, \dots$

For numerical calculations it is useful to resort to the language of second quantization. The Hamiltonian of N particles in second quantization with Fermion creation $\hat{c}_{nm\sigma}^\dagger$ and annihilation $\hat{c}_{nm\sigma}$ operators can be written as:

$$\hat{H} = \sum_{i\sigma} \varepsilon_{i\sigma} \hat{c}_{i\sigma}^\dagger \hat{c}_{i\sigma} + \frac{1}{2} \sum_{ijkl\sigma\sigma'} \langle i, j | \hat{W} | k, l \rangle \hat{c}_{i\sigma}^\dagger \hat{c}_{j\sigma'}^\dagger \hat{c}_{k\sigma'} \hat{c}_{l\sigma}, \quad (5)$$

where the composite index $i = (n, m)$ (similarly j, k, l) denotes the harmonic-oscillator quantum numbers. The Coulomb matrix elements $\langle |\hat{W}| \rangle$ are given explicitly in Ref. [46].

The Hamiltonian (5) conserves total spin, total z -component of spin, $\hat{S}_z = 1/2 \sum_{i\sigma} \sigma \hat{c}_{i\sigma}^\dagger \hat{c}_{i\sigma}$, and total angular momentum, $\hat{L} = \sum_{nm\sigma} (n - m) \hat{c}_{nm\sigma}^\dagger \hat{c}_{nm\sigma}$. Apart from the spin and the geometrical and dynamical symmetries discussed above, the many particle Hamiltonian (5) has also a hidden symmetry related to the separability of the CM and relative motion [7]. The CM symmetry can be expressed by the introduction of new operators describing collective CM excitations of the system:

$$\hat{A}_+^\dagger = \frac{1}{\sqrt{N}} \sum_{nm\sigma} \sqrt{n+1} \hat{c}_{(n+1)m\sigma}^\dagger \hat{c}_{nm\sigma},$$

$$\begin{aligned}
\hat{A}_-^\dagger &= \frac{1}{\sqrt{N}} \sum_{nm\sigma} \sqrt{m+1} \hat{c}_{n(m+1)\sigma}^\dagger \hat{c}_{nm\sigma}, \\
\hat{A}_+ &= \frac{1}{\sqrt{N}} \sum_{nm\sigma} \sqrt{n} \hat{c}_{(n-1)m\sigma}^\dagger \hat{c}_{nm\sigma}, \\
\hat{A}_- &= \frac{1}{\sqrt{N}} \sum_{nm\sigma} \sqrt{m} \hat{c}_{n(m-1)\sigma}^\dagger \hat{c}_{nm\sigma}.
\end{aligned} \tag{6}$$

The operators \hat{A}_+^\dagger and \hat{A}_-^\dagger (\hat{A}_+ and \hat{A}_-) satisfy the following commutation relation with the full interacting Hamiltonian \hat{H} : $[\hat{H}, \hat{A}_\pm^\dagger] = \omega_\pm \hat{A}_\pm^\dagger$ and $[\hat{H}, \hat{A}_\pm] = -\omega_\pm \hat{A}_\pm$. They can be interpreted as creation (annihilation) operators for collective excitations of the system since they increase (decrease) the energy of the system by ω_\pm . They allow for the construction of exact eigenstates of the interacting system.

We can now explicitly define CM operators C which commute with the interacting Hamiltonian:

$$\begin{aligned}
\hat{C}_+ &= \hat{A}_+^\dagger \hat{A}_+ = \frac{1}{N} \sum_{n'm'\sigma'nm\sigma} \sqrt{(n'+1)n} \hat{c}_{(n'+1)m'\sigma'}^\dagger \hat{c}_{n'm'\sigma'} \hat{c}_{(n-1)m\sigma}^\dagger \hat{c}_{nm\sigma}, \\
\hat{C}_- &= \hat{A}_-^\dagger \hat{A}_- = \frac{1}{N} \sum_{n'm'\sigma'nm\sigma} \sqrt{(m'+1)m} \hat{c}_{n'(m'+1)\sigma'}^\dagger \hat{c}_{n'm'\sigma'} \hat{c}_{(m-1)m\sigma}^\dagger \hat{c}_{nm\sigma}.
\end{aligned} \tag{7}$$

Because Slater determinants constructed from a FD basis set are eigenstates of \hat{L} and \hat{S}_z , it is natural to resolve the total angular momentum L and the total spin in z -direction S_z as good quantum numbers. On the other hand, the structure of the operators $\hat{\mathbf{S}}^2$ and \hat{C}_\pm in second quantization is similar to that of the Coulomb interaction, involving two creation and two annihilation operators. In what follows we construct ED methods which make use of these operators to reduce the size of the Hamiltonian matrix.

SPIN-RESOLVED CI METHOD

The form of the total spin operator in the language of creation and annihilation operators is:

$$\hat{\mathbf{S}}^2 = N/2 + \hat{S}_z^2 - \sum_{ij} \hat{c}_{j\uparrow}^\dagger \hat{c}_{i\downarrow}^\dagger \hat{c}_{j\downarrow} \hat{c}_{i\uparrow}. \tag{8}$$

Its last term annihilates one particle in a state i and recreates it on the same orbital, but with flipped spin; the same is true for the orbital j . Thus, the pattern of orbital quantum numbers is conserved, which makes it possible to arrange the Slater determinants in blocks which enclose all states with the same pattern, and to rotate the single blocks into eigenstates

of $\hat{\mathbf{S}}^2$. The size of the blocks can be obtained using combinatoric arguments. We start with a given electron number N , among which N_\uparrow electrons are spin up, and N_\downarrow spin down, and we distribute them on M orbitals ($M \leq N$). Because of Pauli's exclusion principle we get

$$\frac{N}{2} \leq \max(N_\uparrow, N_\downarrow) \leq M \leq N. \quad (9)$$

Thus we have $N - M$ doubly occupied orbitals (singlets), $M - N_\downarrow$ unpaired spins up, and $M - N_\uparrow$ unpaired spins down. The distribution of the singlets is determined by Pauli's principle. The number of different orbitals available for unpaired spins up and unpaired spins down is $M - (N - M)$. The size of the block equals the number of all possible distributions of unpaired electrons spin up and down on $M - (N - M)$ orbitals:

$$\begin{aligned} \text{blocksize} &= \binom{M - (N - M)}{M - N_\downarrow} \binom{M - (N - M) - (M - N_\downarrow)}{M - N_\uparrow} \\ &= \frac{(2M - N)!}{(M - N_\downarrow)!(M - N_\uparrow)!}. \end{aligned} \quad (10)$$

In Table I we show the number of total spin eigenstates per block for a six-electron system as a function of M and $S_z = (N_\uparrow - N_\downarrow)/2$. These blocks are fairly small (e.g., blocksize = 252 for $N = M = 10$, $S_z = 0$) and the diagonalization of the blocks has to be done only once for each value of M .

In Table II we show how the size of the Hamiltonian is reduced by applying the scheme on a system with $N = 5$, $L = 1$, $S_z = 1/2$ and 352954 Slater determinants and on a system with $N = 6$, $L = S_z = 0$ and 326120 Slater determinants. Note that for even electron numbers N the largest subspace is that of $S = 1$, not $S = 0$. In the case of odd N the $S = 1/2$ subspace is larger than the others.

We now apply the spin-resolved CI method to the calculation of the ground state energy of 4 through 7 electrons. The accuracy of the method is assessed by comparison of our calculations in zero magnetic field with available results from quantum Monte Carlo and stochastic-variational method. The calculations were performed using GaAs parameters ($\varepsilon = 12.4$, $m^* = 0.067$) and a confinement energy $\omega_0 = 3.32$ meV. Table III shows the ground state energies for a number of subspaces L , S . We see that the QMC and SVM energies appear to be slightly lower than the ED results, however, their order appears to change depending on the actual subspace and number of electrons. Altogether, the ED appears to give highly reliable results for ground and excited states which can be extended to finite magnetic fields.

	M=3	M=4	M=5	M=6
$S_z = 0$	$S = 0: 1$	$S = 1: 1$	$S = 0: 2, S = 1: 3,$ $S = 2: 1$	$S = 0: 5, S = 1: 9,$ $S = 2: 5, S = 3: 1$
$S_z = \pm 1$		$S = 1: 1$	$S = 1: 3, S = 2: 1$	$S = 1: 9, S = 2: 5,$ $S = 3: 1$
$S_z = \pm 2$			$S = 2: 1$	$S = 2: 5, S = 3: 1$
$S_z = \pm 3$				$S = 3: 1$

TABLE I: Number of total spin eigenstates per block for a six-electron system as a function of M and S_z .

N	$S=1/2$	$S=3/2$	$S=5/2$	Σ
5	184769	137705	30480	352954

N	$S = 0$	$S = 1$	$S = 2$	$S = 3$	Σ
6	92410	152460	70711	10539	326120

TABLE II: Effective size of the Hamiltonian for systems with $N = 5$, $L = 1$, $S_z = 1/2$ and 352954 Slater determinants and with $N = 6$, $L = S_z = 0$ and 326120 Slater determinants.

N	(L, S)	$E_{\text{QMC}}[\text{meV}]$	$E_{\text{SVM}}[\text{meV}]$	$E_{\text{ED}}[\text{meV}]$	rel. error of ED
4	$(0, 1)$	44.0439	44.0261	44.0763	$< 1.2 \cdot 10^{-3}$
4	$(-2, 0)$	44.5301	44.4945	44.5498	$< 1.3 \cdot 10^{-3}$
4	$(0, 0)$	44.8301	44.8004	44.8355	$< 8 \cdot 10^{-4}$
5	$(-1, 1/2)$	65.6159	65.5827	65.6488	$< 10^{-3}$
6	$(0, 0)$	90.1166	90.1391	90.2383	$< 1.5 \cdot 10^{-3}$
7	$(-2, 1/2)$	118.9784	—	119.1426	$< 1.2 \cdot 10^{-3}$
7	$(0, 1/2)$	119.3045	—	119.4069	$< 1.0 \cdot 10^{-3}$

TABLE III: Comparison of ground state energies for $N = 4, 5, 6, 7$ of the subspaces L, S ($\omega = 3.32$ meV) at $B = 0$. QMC energies are from Ref. [33], and SVM energies from Ref. [43]. SVM results for seven electrons are not available.

SPIN- AND CM-RESOLVED CI METHOD

The ED method with both the total spin and the CM resolved as good quantum numbers is particularly applicable in the high magnetic field strongly correlated regime, where correlation effects dominate the reconstruction of the dot through magic states [6, 20, 48], spin textures [21], and skyrmions [10].

The construction starts with defining the number of electrons N and their total angular momentum L . Moreover, we restrict the single-particle basis set by choosing the number of Landau levels of interest. This is done by fixing the maximal quantum number n_{\max} . Since the total angular momentum is defined using the FD numbers n and m , the above choices impose a limitation on the number m , i.e., determine an m_{\max} such that $\sum_{j=1}^N m_j = \sum_{j=1}^N n_j - L \leq n_{\max}N - L \leq m_{\max}$. The Hilbert space is thus finite and we can generate all configurations and diagonalize them with respect to the CM and total spin operators. Since we restrict ourselves to n_{\max} Landau levels, only the CM operator \hat{C}_- is of interest. From its definition (Eq. (7)) we see that \hat{C}_- increases/decreases the quantum number m , but does not change the pattern of numbers $n\sigma$. We can therefore organize our configurations in blocks with the same $n\sigma$ pattern; these blocks are diagonalized separately. The general scheme is thus similar to that for the total spin, only here the CM diagonalization has to be done for each block as the matrix elements of \hat{C}_- in second quantization explicitly depend on m . We retain only the eigenstates with eigenvalue $C_- = 0$, because the eigenstates corresponding to eigenvalues 1, 2, 3, .. can be generated systematically by applying the CM motion creation operator \hat{A}_-^\dagger on eigenstates with eigenvalue 0.

Our next aim is to resolve the total spin in the basis of stored CM eigenvectors. We have established that $\hat{\mathbf{S}}^2$ couples states with the same nm pattern. It is therefore convenient to introduce superblocks with the same n pattern. Thus, a superblock encloses all blocks with the same $n\sigma$ pattern and $\hat{\mathbf{S}}^2$ can couple states only within a superblock. After calculating all eigenstates with zero CM motion in the previous step, all states with the same n pattern are collected and diagonalized with respect to the total spin operator $\hat{\mathbf{S}}^2$. Note that one set of CM eigenvectors calculated for the system with lowest possible spin polarization (0 for even number of electrons, 1/2 for odd number of electrons) can be used to calculate all possible eigenvalues of $\hat{\mathbf{S}}^2$. As a result we obtain a basis set consisting of eigenstates of the operators \hat{L} , \hat{S}_z , $\hat{\mathbf{S}}^2$, and \hat{C}_- , which we use to generate the Hamiltonian matrix. Table IV shows how

the Hilbert space is reduced for the $(S_z, L) = (0, -18)$ subspace of a four-electron system in the two-Landau-level approximation ($n_{\max} = 1$). The first column labels the superblocks. The second column contains the information which electrons are in the lowest ($n = 0$), and which are in the second Landau level ($n = 1$), and how many configurations are possible (third column). Each superblock may enclose several blocks which are labelled in the fourth column. The $n\sigma$ -pattern and the corresponding number of configurations are in the fifth and sixth columns. After applying the CM operator and filtering out states with zero CM motion the number of states is reduced for each $n\sigma$ block (seventh column), and to 1555 in total (see last row). In the next step all superblocks are diagonalized with respect to the total spin operator. The resulting numbers of configurations for $S = 0, 1$, and 2 are given in the last column. Thus, instead of having to solve an eigenvalue problem of the size 15456 in the subspace $S_z = 0, L = -25$ we end up with three eigenvalue problems with matrix sizes 528, 791, and 236 (see last row). To illustrate the method and compare it with previous work [2, 6, 7, 8, 10, 13, 15, 49] we show the results for four electrons in the range of magnetic fields $0 - 8$ T for GaAs parameters ($\varepsilon = 12.4$, $m^* = 0.067$), confinement energy $\omega_0 = 3$ meV, and one and two Landau levels. In Fig. 1 we show the energies of the ground and the two lowest-lying excited states of each subspace L, S with $C_- = 0$, without the Zeeman energy ($g = 0$). The spectrum in Fig. 1 exhibits an energy band consisting of ground states of all S -subspaces, is separated from the excited states by $\Delta E \approx 0.6$ meV (marked by the double arrow). Since the energy needed to construct an excitation of the CM motion is of the same order of magnitude ($\omega_- = 0.62$ meV for 8 T and higher for smaller magnetic fields), this separation clearly shows that the lowest-lying excited states of the quantum dot for magnetic field between 4 and 8 T are all excitations of the relative motion.

In Fig. 2 we show the evolution of the ground state energy with the magnetic field in the one- and two-Landau-level approximation with GaAs Zeeman energy ($g = -0.44$). In the one-Landau-level approximation we do not find the Hund's rule state expected at $B = 0$ nor the $\nu = 2$ spin-singlet droplet with $S = 0, L = -2$. The first quantum Hall state is the spin-polarized state with $S = 2, L = -6$. Starting at $B = 4$ T we find the reconstruction of the $\nu = 1$ droplet. This correlation-driven effect is expressed in a number of ground state transitions with decreasing angular momentum (Fig. 2(a), (b)). The ground states change both angular momentum and spin, in agreement with previous work [2, 6, 7, 8, 10, 13, 15, 49]. In Fig. 2(b) we show the evolution of the ground state in the two-Landau-level

Superblock	n pattern	Size	Block	$n\sigma$ pattern	Size	$C_- = 0$	Spin resolved
1	(0, 0, 0, 0)	728	a	(0 \downarrow , 0 \downarrow , 0 \uparrow , 0 \uparrow)	728	78	$S = 0$: 26 $S = 1$: 42 $S = 2$: 10
2	(0, 0, 0, 1)	3458	a	(0 \downarrow , 0 \downarrow , 0 \uparrow , 1 \uparrow)	1729	182	$S = 0$: 126
			b	(0 \downarrow , 1 \downarrow , 0 \uparrow , 0 \uparrow)	1729	182	$S = 1$: 182 $S = 3$: 56
3	(0, 0, 1, 1)	5880	a	(0 \downarrow , 0 \downarrow , 1 \uparrow , 1 \uparrow)	910	91	$S = 0$: 196
			b	(0 \downarrow , 1 \downarrow , 0 \uparrow , 1 \uparrow)	5880	406	$S = 1$: 301
			c	(1 \downarrow , 1 \downarrow , 0 \uparrow , 0 \uparrow)	910	91	$S = 2$: 91
4	(0, 1, 1, 1)	4270	a	(0 \downarrow , 1 \downarrow , 1 \uparrow , 1 \uparrow)	2135	210	$S = 0$: 145
			b	(1 \downarrow , 1 \downarrow , 0 \uparrow , 1 \uparrow)	2135	210	$S = 1$: 210 $S = 2$: 65
5	(1, 1, 1, 1)	1120	a	(1 \downarrow , 1 \downarrow , 1 \uparrow , 1 \uparrow)	1120	105	$S = 0$: 35 $S = 1$: 56 $S = 2$: 14
Σ		15456			15456	1555	$S = 0$: 528 $S = 1$: 791 $S = 2$: 236

TABLE IV: Reduction of the Hilbert space for the $(S_z, L) = (0, -25)$ subspace of a four-electron system in the two-Landau-level approximation using CM and total spin as good quantum numbers.

approximation. We still miss the Hund's rule $B = 0$ state, but recover the $\nu = 2$ state with $L = -6$ and $S = 0$.

The qualitative agreement between the lowest- (Fig. 2(a)) and two-Landau-level (Fig. 2(b)) approach is good for high magnetic fields, i.e., beyond the $\nu = 1$ quantum Hall droplet. The only difference is the $(S, L) = (0, -8)$ phase which is present in Fig. 2(a), and missing in Fig. 2(b). The absence of the low-spin phase is due to the weakening of Coulomb interactions by inclusion of higher Landau levels. The second effect is that the fields corresponding to the ground-state transitions are lower in the one-Landau-level due

to the fact that in this approximation the correlation effects are underestimated.

An advantage of the CI method over QMC and SVM methods is the ability to calculate excited states. In Fig. 3 we show the energy gap between the ground and the lowest-lying excited states as a function of the magnetic field and Zeeman energy for the $N=4$ electron system, calculated in the two-Landau-level approximation. The magnetic field changes from 0 to 10.5 T, where the filling factor $\nu = 1/3$ -droplet (angular momentum -18) emerges. In Fig. 3(a) we plot the energy gap between the ground state and the lowest excited state with the same S_z (selection rule $\Delta S_z = 0$, without restrictions for the quantum numbers L, S). This selection rule applies to charge excitations. Consequently, we cannot expect a systematic increase of the gap as a function of the Zeeman energy. All the structures in the diagram for increasing Zeeman energy are caused by transitions to higher polarized states. In contrast, we used the selection rule $\Delta S_z = \pm 1$ for Fig. 3(b). This kind of excitation should be observed in microwave-radiation or in spin-flip-Raman experiments. The characteristic features in this case are energy gaps linearly growing with Zeeman energy. This behavior is especially pronounced in the regime of the $\nu = 1$ droplet around $B = 3$ T and in the regime of the $\nu = 1/3$ droplet around $B = 10$ T, where both ground and first excited state are stable.

CONCLUSIONS

We presented a configuration interaction method optimized for Fock-Darwin states of two-dimensional quantum dots with an axially symmetric parabolic confinement potential subject to perpendicular magnetic field. The optimization explicitly accounts for geometrical and dynamical symmetries of Fock-Darwin single-particle states and for many-particle symmetries associated with the center-of-mass motion and with total spin. As a key element we introduced a block structure to cluster Slater determinants which are coupled by $\hat{\mathbf{S}}^2$ and/or \hat{C}_- . By diagonalizing these small blocks we managed to rotate the many-particle basis set into eigenstates of $\hat{\mathbf{S}}^2$ and/or \hat{C}_- , and used them to calculate the Hamiltonian matrix. This reduced the size of the basis set and increased the accuracy of exact diagonalization calculations for quantum dots. The results compare well with available quantum Monte-Carlo and stochastic-variational results. Thus we show that the CI method gives reliable results for the ground and excited states and allows to study the effects of electron correlation and the

magnetic field over a broad range of system parameters. It is intended to serve as a benchmark for other methods which can be extended to larger particle numbers.

ACKNOWLEDGEMENT

A. W. thanks the German Academic Exchange Service (Grant no. D/00/05486), the RRZE Erlangen, and the Institute for Microstructural Sciences, National Research Council of Canada for financial support and hospitality.

- [1] L. Jacak, P. Hawrylak, and A. Wojs, *Quantum Dots* (Springer, Berlin, 1998).
- [2] P.A. Maksym and T. Chakraborty, Phys. Rev. Lett. **65**, 108 (1990).
- [3] U. Merkt, J. Huser, and M. Wagner, Phys. Rev. B **43**, 7320 (1991).
- [4] D. Pfannkuche, V. Gudmundsson, and P.A. Maksym, Phys. Rev. B **47**, 2244 (1993).
- [5] P. Hawrylak and D. Pfannkuche, Phys. Rev. Lett. **70**, 485 (1993).
- [6] S.-R. Eric Yang, A.H. MacDonald, and M.D. Johnson, Phys. Rev. Lett. **71**, 3194 (1993).
- [7] P. Hawrylak, Phys. Rev. Lett. **71**, 3347 (1993).
- [8] J.J. Palacios, L. Martin-Moreno, G. Chiappe, E. Louis, and C. Tejedor, Phys. Rev. B **50**, 5760 (1994).
- [9] A. Wojs and P. Hawrylak, Phys. Rev. B **51**, 10880 (1995).
- [10] J.H. Oaknin, L. Martin-Moreno, J.J. Palacios, and C. Tejedor, Phys. Rev. Lett. **74**, 5120 (1995).
- [11] A. Wojs and P. Hawrylak, Phys. Rev. B **53**, 10841 (1996).
- [12] P.A. Maksym, Phys. Rev. B **53**, 10871 (1996).
- [13] P. Hawrylak, A. Wojs, and J.A. Brum, Phys. Rev. B **54**, 11397 (1996).
- [14] A. Wojs and P. Hawrylak, Phys. Rev. B **55**, 13066 (1997).
- [15] A. Wojs and P. Hawrylak, Phys. Rev. B **56**, 13227 (1997).
- [16] M. Eto, Jpn. J. Appl. Phys. **36**, 3924 (1997).
- [17] M. Eto, J. Phys. Soc. Japan **66**, 2244 (1997).
- [18] P.A. Maksym, Physica B **249-251**, 233 (1998).
- [19] H. Imamura, H. Aoki, and P.A. Maksym, Phys. Rev. B **57**, R4257 (1998).

- [20] H. Imamura, H. Aoki, and P.A. Maksym, *Physica B* **249-251**, 214 (1998).
- [21] P. Hawrylak, C. Gould, A.S. Sachrajda, Y. Feng, and Z. Wasilewski, *Phys. Rev. B* **59**, 2801 (1999).
- [22] C.E. Creffield, W. Häusler, J.H. Jefferson, and S. Sarkar, *Phys. Rev. B* **59**, 10719 (1999).
- [23] N.A. Bruce and P.A. Maksym, *Phys. Rev. B* **61**, 4718 (2000).
- [24] S.M. Reimann, M. Koskinen, and M. Manninen, *Phys. Rev. B* **62**, 8108 (2000).
- [25] S.A. Mikhailov, *Phys. Rev. B* **65**, 115312 (2002).
- [26] F. Bolton, *Phys. Rev. B* **54**, 4780 (1996).
- [27] A. Harju, V.A. Sverdlov, R.M. Nieminen, and V. Halonen, *Phys. Rev. B* **59**, 5622 (1999).
- [28] A. Harju, S. Siljamäki, and R.M. Nieminen, *Phys. Rev. B* **60**, 1807 (1999).
- [29] A. Harju, S. Siljamäki, and R.M. Nieminen, *Phys. Rev. B* **65**, 075309 (2002).
- [30] A. Harju, S. Siljamäki, R.M. Nieminen, V.A. Sverdlov, and P. Hyvönen, *Phys. Rev. B* **65**, 121306 (2002).
- [31] R. Egger, W. Häusler, C.H. Mak, and H. Grabert, *Phys. Rev. Lett.* **92**, 3320 (1999).
- [32] F. Pederiva, C.J. Umrigar, and E. Lipparini, *Phys. Rev. B* **62**, 8120 (2000).
- [33] F. Pederiva, C.J. Umrigar, and E. Lipparini, *Phys. Rev. B* **68**, 089901 (2003).
- [34] A.V. Filinov, M. Bonitz, and Y.E. Lozovik, *Phys. Rev. Lett.* **86**, 3851 (2001).
- [35] C. Yannouleas and U. Landman, *Phys. Rev. Lett.* **82**, 5325 (1999).
- [36] B. Reusch, W. Häusler, and H. Grabert, *Phys. Rev. B* **63**, 113313 (2001).
- [37] M. Koskinen, M. Manninen, and S.M. Reimann, *Phys. Rev. Lett.* **79**, 1389 (1997).
- [38] D.G. Austing, S. Sasaki, S. Tarucha, S.M. Reimann, M. Koskinen, and M. Manninen, *Phys. Rev. B* **60**, 11514 (1999).
- [39] K. Hirose and N.S. Wingreen, *Phys. Rev. B* **59**, 4604 (1999).
- [40] O. Steffens and M. Suhrke, *Phys. Rev. Lett.* **82**, 3891 (1999).
- [41] A. Wensauer, O. Steffens, M. Suhrke, and U. Rössler, *Phys. Rev. B* **62**, 2605 (2000).
- [42] A. Wensauer, J. Kainz, M. Suhrke, and U. Rössler, *phys. stat. sol. (b)* **224**, 675 (2001).
- [43] K. Varga, P. Navratil, J. Usukura, and Y. Suzuki, *Phys. Rev. B* **63**, 205308 (2001).
- [44] V. Fock, *Z. Phys.* **47**, 446 (1928).
- [45] C.G. Darwin, *Proc. Cambridge Phil. Soc.* **27**, 86 (1931).
- [46] P. Hawrylak, *Solid State Commun.* **88**, 475 (1993).
- [47] K. Capelle and G. Vignale, *Phys. Rev. B* **65**, 113106 (2002).

- [48] T. Chakraborty, *Comments Conde. Matt. Phys.* **16**, 35 (1992).
- [49] S.M. Reimann, M. Koskinen, M. Manninen, and B.R. Mottelson, *Phys. Rev. Lett.* **83**, 3270 (1999).

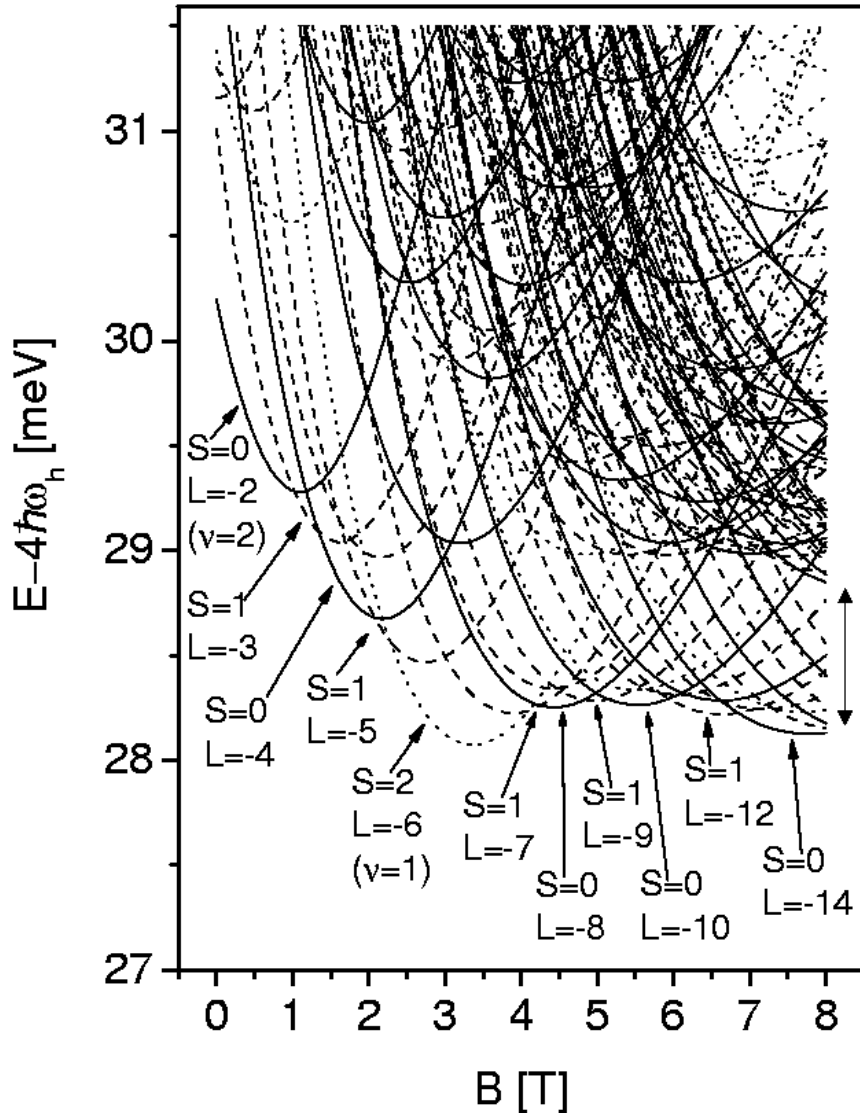


FIG. 1: Energies of the ground state and the two lowest-lying excited states of four electrons with angular momenta $L = -25$ to 0 calculated in the two-Landau-level approximation. The confinement energy is $\omega = 3$ meV and the Zeeman energy is neglected. All these states are eigenstates of the center-of-mass operator with the quantum number $C_- = 0$; solid lines correspond to total spin for $S = 0$, dashed lines - to $S = 1$, and dotted lines to $S = 2$.

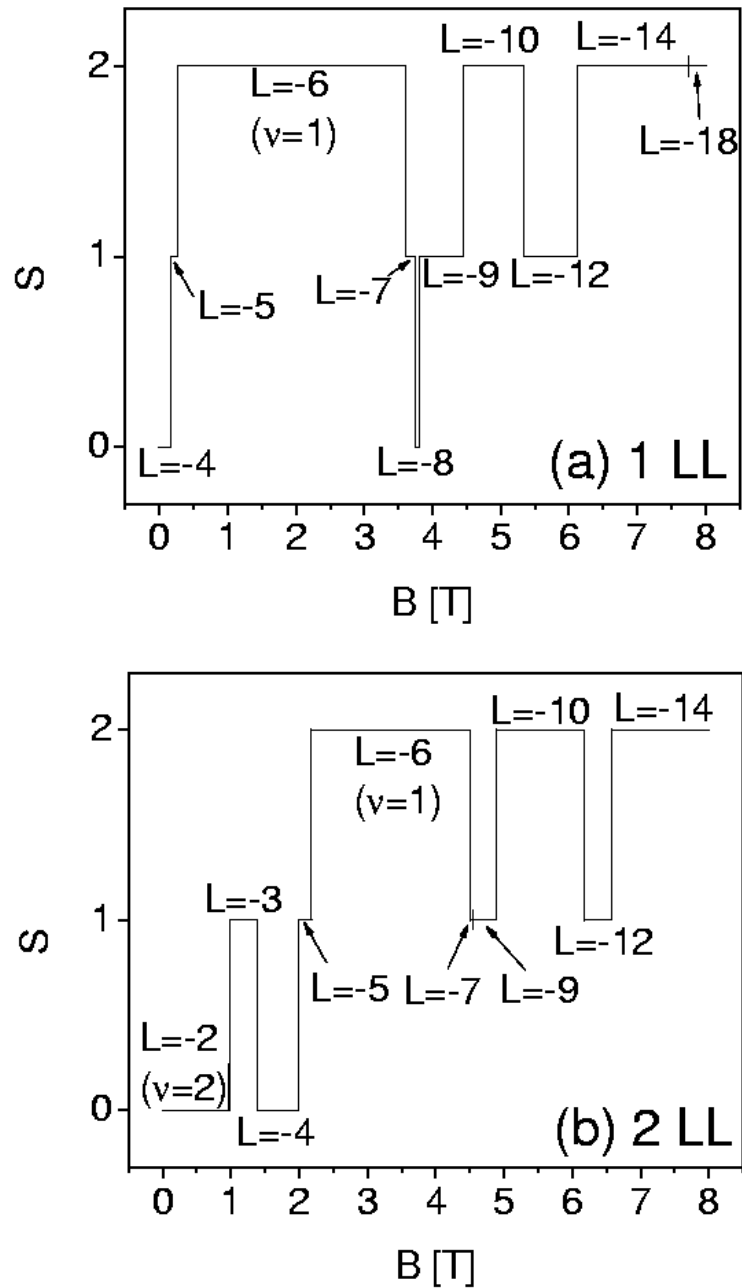


FIG. 2: Phase diagrams for a four-electron system with confinement energy 3 meV and GaAs Zeeman energy ($g = -0.44$) as a function of the magnetic field from 0 to 8 T in one-Landau-level (a) and two-Landau-level approximation (b).

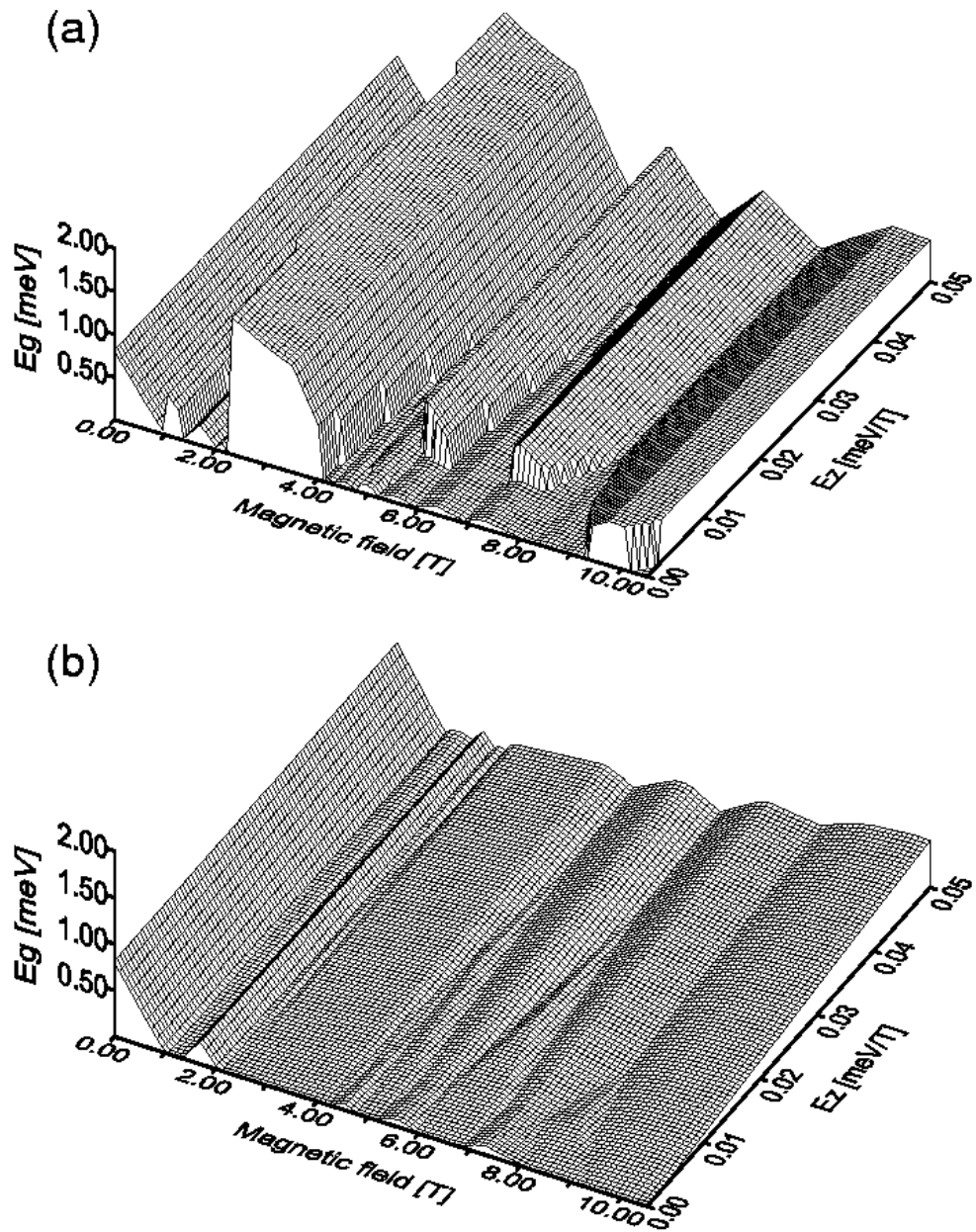


FIG. 3: Energy gap between the ground and the lowest-lying excited state with the same S_z (a) and with $\Delta S_z = \pm 1$ (b) for a four-electron system as a function of magnetic field and Zeeman energy.